Optical Engineering

SPIEDigitalLibrary.org/oe

Blind guidance system based on laser triangulation

Jih-Huah Wu
Jinner-Der Wang
Wei Fang
Yun-Parn Lee
Yi-Chia Shan
Hai-Ko Kao
Shih-Hsin Ma
Joe-Air Jiang

Optical Engineering 51(5), 054302 (May 2012)

Blind guidance system based on laser triangulation

Jih-Huah Wu
Ming Chuan University
Department of Biomedical Engineering
Taoyuan 333, Taiwan

Jinner-Der Wang
St. John's University
Department of Computer Science and Information Engineering
New Taipei City 25135, Taiwan

Wei Fang
National Taiwan University
Department of Bio-Industrial Mechatronics Engineering
Taipei 10617, Taiwan

Yun-Parn Lee
Ming Chuan University
Department of Electronic Engineering
Taoyuan 333, Taiwan

Yi-Chia Shan
National Taiwan University
Department of Bio-Industrial Mechatronics Engineering
Taipei 10617, Taiwan

Hai-Ko Kao
St. John's University
Department of Computer Science and Information Engineering
New Taipei City 25135, Taiwan

Shih-Hsin Ma
Feng Chia University
Department of Photonics
Taichung 40724, Taiwan

Joe-Air Jiang
National Taiwan University
Department of Bio-Industrial Mechatronics Engineering
Taipei 10617, Taiwan
E-mail: jajiang@ntu.edu.tw

Abstract. We propose a new guidance system for the blind. An optical triangulation method is used in the system. The main components of the proposed system comprise of a notebook computer, a camera, and two laser modules. The track image of the light beam on the ground or on the object is captured by the camera and then the image is sent to the notebook computer for further processing and analysis. Using a developed signal-processing algorithm, our system can determine the object width and the distance between the object and the blind person through the calculation of the light line positions on the image. A series of feasibility tests of the developed blind guidance system were conducted. The experimental results show that the distance between the test object and the blind can be measured with a standard deviation of less than 8.5% within the range of 40 and 130 cm, while the test object width can be measured with a standard deviation of less than 4.5% within the range of 40 and 130 cm. The application potential of the designed system to the blind guidance can be expected. [DOI: 10.1117/1.OE.51.5.054302]

Subject terms: blind-guidance system; laser module; optical triangulation.

Paper 111594P received Dec. 18, 2011; revised manuscript received Mar. 7, 2012; accepted for publication Mar. 9, 2012; published online May 7, 2012.

1 Introduction

Three common methods are used in laser range finders: time of flight, triangulation, and phase difference. Triangulation and vision detection are wildly utilized in industrial applications. For example, some automotive systems use optical triangulation to measure the distance between a host vehicle and a preceding vehicle.[1,2] When an active emitter sends a laser to a target, the reflected light goes through the center of the lens and is then mapped onto the image sensor. The combination of the centroid method and laser optics can improve sub-pixel accuracy in various types of image featuring applications, such as one spot or one stripe approaches used in sub-pixel measurement of three-dimensional (3-D) surfaces.[3] Furthermore, the performance of the centroid method for range finders, 3-D measurements, target tracking,[4] and star trackers[5] has been systematically investigated. A two-beam laser triangulation method has also been proposed to measure the position of a moving object.[6] This method uses two parallel laser beams to determine the

0091-3286/2012/$25.00 © 2012 SPIE

moving direction of an object and then track and measure its positions. A novel approach of modeling and calibration of an active laser beam-scanning triangulation measurement system was proposed.[7] In addition, a multi-beam laser probe for measuring position and direction of freeform surface was proposed by Lee.[8]

Some guidance methods and appliances have been used to guide the blind. Blind guidance systems can be categorized into two groups: passive methods and active methods. The passive methods refer to the assisting techniques such as a special pattern brick on the sidewalk used for guidance or a voice message broadcast through the speaker located at an intersection. The active methods, on the other hand, can be exemplified as a wearable apparatus designed for the blind[9] or an electronic blind cane[10,11] that uses a supersonic method to actively detect the environment. In some cases, apparatuses integrate with GPS and the electronic map to guide the direction and location to the blind. Another type of active apparatus is the mobile robot,[12] which is capable of guiding the blind but with high costs. Moreover, a guide device for blind people was proposed by Ban and Mitsuta.[13] The distance information of Ban and Mitsuta's devise is dependent on the energy variation received by the photoelectric element. However, this device is less reliable. It cannot accurately measure the distance between the blind person and the obstacle, nor can it offer the terrain information to the blind person.

In this paper, a blind guidance system based on optical triangulation is proposed to help the blind detect both the obstacle and terrain information. The distance measurement accuracy of the proposed blind guidance system was examined. Our experimental results also validate the feasibility of the system.

2 Measurement Principle

2.1 *System Architecture*

The proposed system uses a cross-plane method to detect the environment in front of the blind. The optical principle is based on the triangulation method, using lasers and a camera to conduct the detection task. The main components of the proposed system comprise a notebook computer, a camera, and two laser modules. One of the laser modules emits a light beam on the vertical axis to detect the front situation. The other laser module emits a light beam on the tilted horizontal axis to detect the plane with a tilted angle. In order to reduce the power consumption, the laser modules are switched on/off with a trigger pulse. Also, in order to decrease the computation complexity, the two laser modules are switched on alternately. The system architecture is shown in Fig. 1. The proposed appliance can be girded around the chest of the blind person, and the whole setup of the system is illustrated in Fig. 2. The designed guidance system includes a notebook-computer, a camera, a filter, and two laser modules. These two laser modules are in the same height, as shown in Fig. 3. The width of the object and the distance between the object and the blind can be calculated by the system that we proposed.

In the system, the visible laser with a central wavelength of 650 nm and output power of 3 mW is used. The visible light can be easily detected in the experiment. In the future application, the laser light will be changed to a non-visible light. One of the laser modules emits the tilted horizontal beam of lights. The purpose of such a design is to detect the path situation below the user's waist and measure the distance from the user to the obstacle and the obstacle width. The other vertical laser module emits a vertical beam of lights. It can detect the ground situation in front of the blind. A cylindrical lens is inserted in the front part of the laser module. Using the cylindrical lens, a point of light can be transformed into a beam of light. The resolution camera adopted in the system is 640×480 pixels (width $\times$ height). The track of the light line beam is captured by the camera, and the image is sent to the notebook computer for computation. Moreover, a bandpass filter is mounted in the front part of the sensor such that the lights can be filtered out except for the specific laser light. This means that the filter can increase the signal-to-noise ratio in image processing. The central wavelength and bandwidth of the adopted filter are 650.88 and 43.62 nm, respectively. A microprocessor module (EM1206, manufactured by Tibbo Technology Inc.) is used to control laser modules on/off alternately via a serial port. The purpose of using the EM1206 is to reduce the power consumption and the processing time. In our experiment, a test carton is used as an obstacle. The dimension of the carton (length $\times$ width $\times$ height) is $36 \times 28 \times 6$ cm^3.

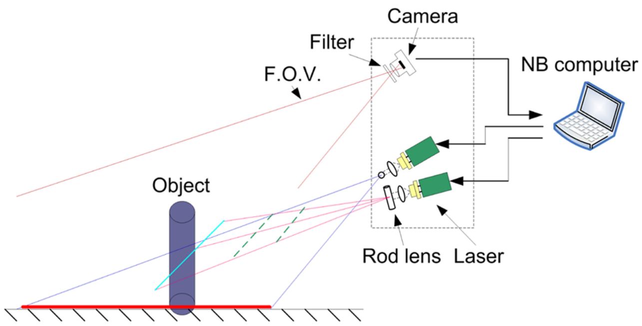

Fig. 1 The architecture of the proposed guidance system.

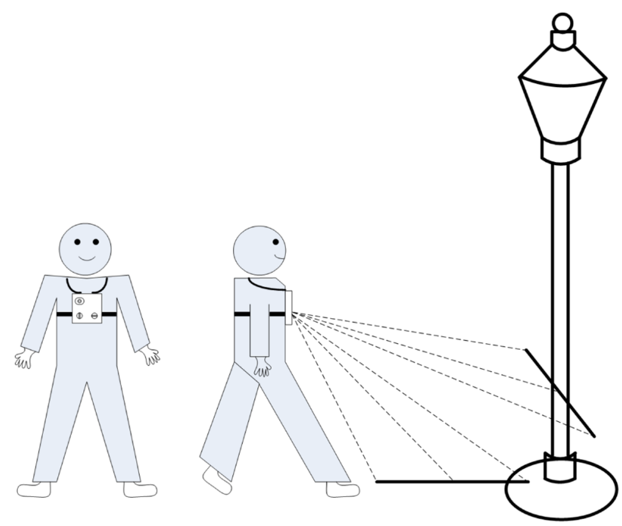

Fig. 2 Application illustration of girding the proposed guidance system around the blind person's chest.

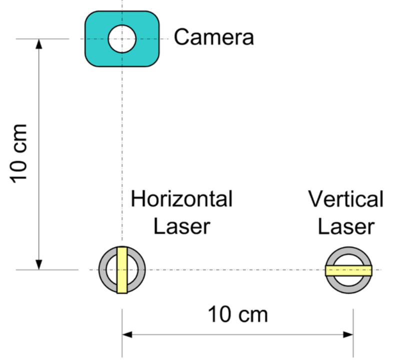

Fig. 3 Front view of the components arrangement of the proposed guidance system.

2.2 *Methods for Distance Measurement*

The setup of the proposed appliance is shown in Fig. 2. It can be used to detect horizontal and vertical situations. The front view of the installation profile is shown in Fig. 3; there are a camera and two laser modules. The camera and the laser modules are 10 cm apart, and the heights of the two laser modules are the same.

An optical triangulation method is used in the designed guidance system to measure the distance ranging from 40 to 130 cm. There are two methods proposed in this study to measure the distance: one is the ideal formula and the other is the LUT (look-up-table) method. In the ideal formula, the measurement distance can be calculated by the equations developed in Sec. 2.3, but the optical aberration effect and mechanical error will affect the measurement accuracy. To cope with the mentioned problem, the LUT method (including calibration) is also adopted in this study. To this end, the database regarding the position detected by the image sensor and the real distance will be established. First of all, we make some benchmarks on the ground, ranging from 40 to 140 cm, by using the guidance system. Then the real distance can be calculated by the LUT method according to the position detected by the image sensor. If the position detected by the image sensor is beyond the estimation of the LUT, the distance can be estimated by the interpolation algorithm.

2.3 *Derivation of Distance Estimation Formula*

2.3.1 *Horizontal optical triangulation-based method*

Calculation of the distance $\boldsymbol{Z}$. The horizontal laser beam is used to find the distance Z between the object and the laser. The geometrical layout is shown in Fig. 4. For a concise reason, the filter is omitted here. θ is the tilted angle of the camera (includes the lens and the sensor), and α is the tilted angle of the horizontal laser. When the horizontal laser module emits a beam of lights, it is captured by the camera. The Q point of the object is projected onto the image sensor, and the position of the projected point on the image sensor is separated by distance d from the optical axis.

Based on the trigonometry, Eq. (1) is obtained from the triangle G-Q-F when $Q > E$.

$$\tan\left(\frac{\pi}{2} - \theta + \beta\right) = \frac{Z}{D + Z \times \tan\alpha}. \tag{1}$$

Otherwise, the sign in front of the angle β will be negative, when $Q < E$. In Eq. (1), D is the height from the horizontal laser to the lens. This distance D is 10 cm and remains a constant in the design. Z is the distance between the point-Q and point-F, and the height from the point-F to the point-L will be $Z \times \tan(\alpha)$. And the height of the image sensor from the ground is H (120 cm) in this system.

The distance Z can be derived according to the geometric layout shown in Fig. 4 and is given as

$$Z = \frac{D \times \tan\left(\frac{\pi}{2} - \theta + \beta\right)}{1 - \tan\alpha \times \tan\left(\frac{\pi}{2} - \theta + \beta\right)}. \tag{2}$$

According to the thin-lens equation, if the object distance is larger, the image distance I is approximately equal to the focal length f of the lens. Then tan (β) can be approximately equal to d/f. After rearranging Eq. (2), the distance Z can be obtained as follows:

$$Z \cong \frac{D(f + d\tan\theta)}{f(\tan\theta - \tan\alpha) - d(1 + \tan\theta\tan\alpha)}. \tag{3}$$

Calculation of the object width $\boldsymbol{X}_1$. Figure 5 is the BB-view of Fig. 4. After the distance Z is acquired, the object width X_1 can be further estimated. X_2 is the distance between the two ends of the light line on the camera sensor, L_1 is the distance from the object to the lens, and L_2 is the image distance from the lens to the image spot.

Using the ratio principle from Figs. 4 and 5, we can get Eq. (4).

$$\frac{X_1}{X_2} = \frac{L_1}{L_2} = \frac{\dfrac{Z}{\sin\left(\frac{\pi}{2} - \theta + \beta\right)}}{\sqrt{d^2 + I^2}} \cong \frac{\dfrac{Z}{\sin\left(\frac{\pi}{2} - \theta + \beta\right)}}{\sqrt{d^2 + f^2}}. \tag{4}$$

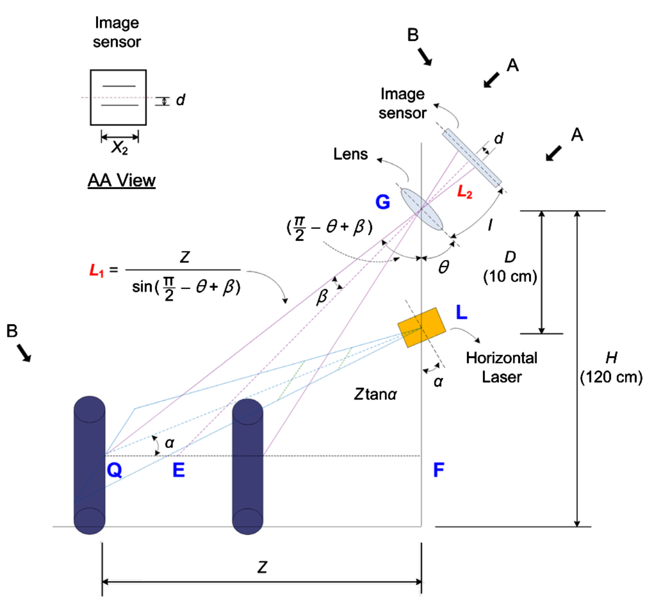

Fig. 4 The geometrical layout for the horizontal laser beam profile of the proposed guidance system.

The object width X_1 can be obtained approximately by

$$X_1 \cong \frac{ZX_2}{(\cos\theta\cos\beta + \sin\theta\sin\beta)(\sqrt{d^2+f^2})}. \tag{5}$$

Since the tan β is approximately equal to d/f, X_1 can be further simplified to

$$X_1 \cong \frac{ZX_2}{f\cos\theta + d\sin\theta}. \tag{6}$$

2.3.2 *Vertical optical triangulation-based method*

The vertical laser beam is used to detect the vertical situation, such as the front and terrain situations. Figure 6 is the upstairs detection profile, and the downstairs detection profile is omitted here for a concise reason. From Fig. 3, the vertical laser line and the camera are not on the same vertical axis, so the light beam will not be a straight line on the image sensor. Figure 6 shows that the separation between vertical laser and camera is 10 cm, so that when the blind goes upstairs and the laser illuminates forward, some turning points will appear at the stairs. On the contrary, when the blind goes downstairs, breakpoint occurs on the stairs. By using the trigonometry illustrated in Fig. 6, the distance L from the transition point (point-K) to the position of the system (point-F) can be calculated.

Based on the triangle G-K-F, the distance L is derived as

$$L = \frac{H}{\tan(\theta+\beta')}, \tag{7}$$

where the angle β' is defined in Fig. 6. And the $\tan(\beta')$ is d/I, which can be approximately equal to d/f, so the distance L can be obtained by following formula:

$$L \cong \frac{H(f - d\tan\theta)}{(f\tan\theta + d)}. \tag{8}$$

2.4 *The LUT Method*

First, the LUT method is utilized to record the data regarding the position detected by the image sensor and the real distance ranging from 40 to 130 cm. Two LUTs are generated when the horizontal laser (tilted angle) applications are employed. One shows the relationship between the image position and the distance, and the other demonstrates the relationship between the image line segment and the width of the object. By contrast, only one LUT is created by the vertical laser application. This LUT reveals the relationship between the image position and the distance of the object (raised or dented stairs). The distance and the object's width can be calculated with the program that we proposed.

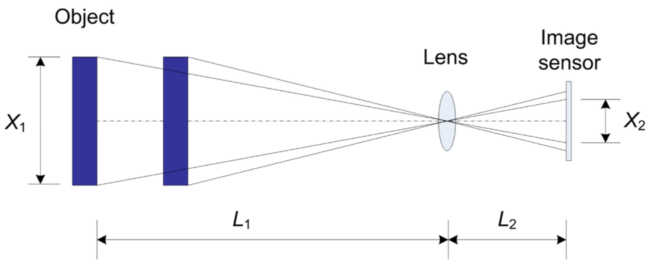

Fig. 5 BB-view on the horizontal laser line profile of the proposed guidance system.

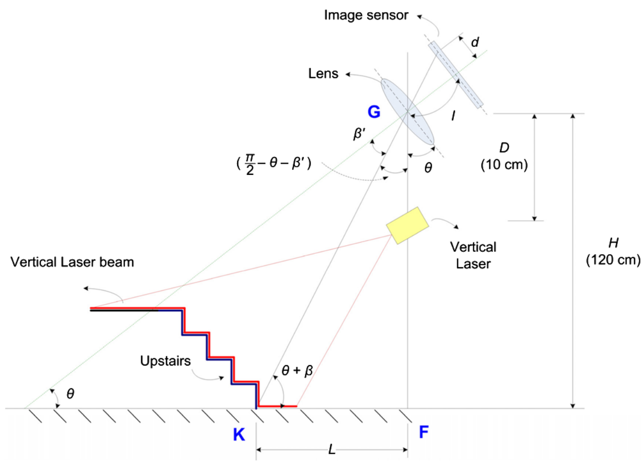

Fig. 6 The geometrical layout for upstairs situation on the vertical laser line of the proposed guidance system.

The signal-processing flowchart is shown in Fig. 7. When the program starts, the camera will be turned on. First of all, the guidance system detects the situation using the vertical laser through the steps of turning on the vertical laser, capturing an image frame, and turning off the vertical laser. Next the taken image will be processed by the program that we designed, including the conversion of a color image to a grayscale image, threshold processing, and thinning processing. Due to the obstacles or the influences of terrain, the laser beam may be deviated. The proposed system can estimate the distance of the first raised position or the dented position from the blind person and count the number of the raised points and the dented points. After completing data processing obtained from vertical laser, the system will estimate the distance Z and the obstacle width X_1 using the tilted horizontal laser. The horizontal laser works the same way as the vertical laser during the detection. The taken image will also be processed by the program that we designed, including the conversion of a color image to a grayscale image, threshold processing, and the centric method. To this end, the distance and the obstacle width can be accurately estimated by the proposed system. After finishing all of the processing, the guidance system will inform the users the results by screen messages and voice prompts.

3 Experimental Results

The specification of the camera is 640×480 pixels (width $\times$ height). The pixel dimension of the camera is 5.6×5.6 μm^2. The focal length of the lens is 4.5 mm. The setup angle θ of the camera is 52 deg, and the setup angle α of the camera is 33.6 deg. Before conducting the experimental measurement, the benchmarks were drawn on the ground in different positions, which is ranged from 40 to 140 cm and serves as reference for evaluating the performance of the guidance system, as shown in Fig. 8. The Cartesian coordinate system is used on the image; X-axis is on the horizontal side, and Y-axis is on the vertical side. The coordinates of the original point (top left) on the

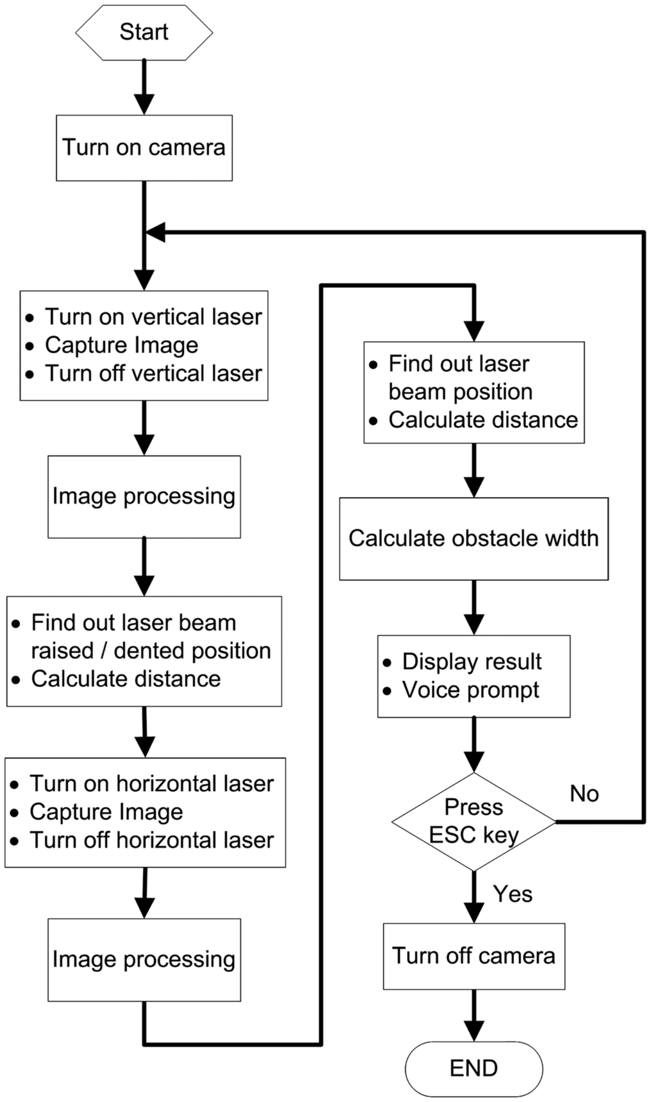

Fig. 7 The signal-processing flowchart adopted in the proposed guidance system.

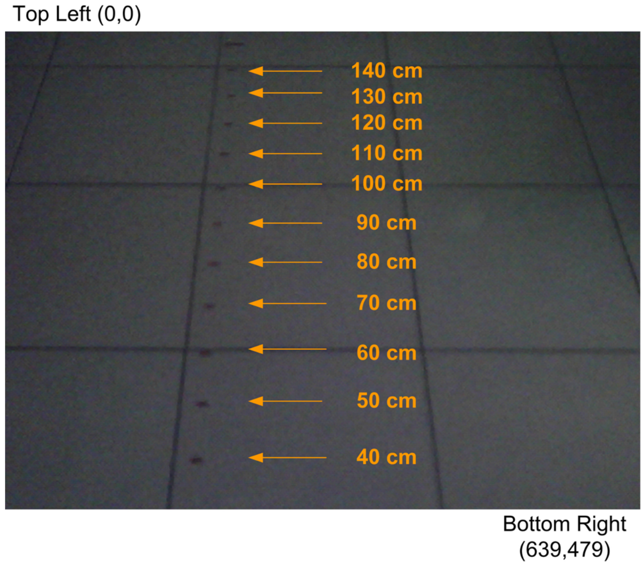

Fig. 8 Benchmarks marked on the ground as reference for evaluating performance of the proposed guidance system.

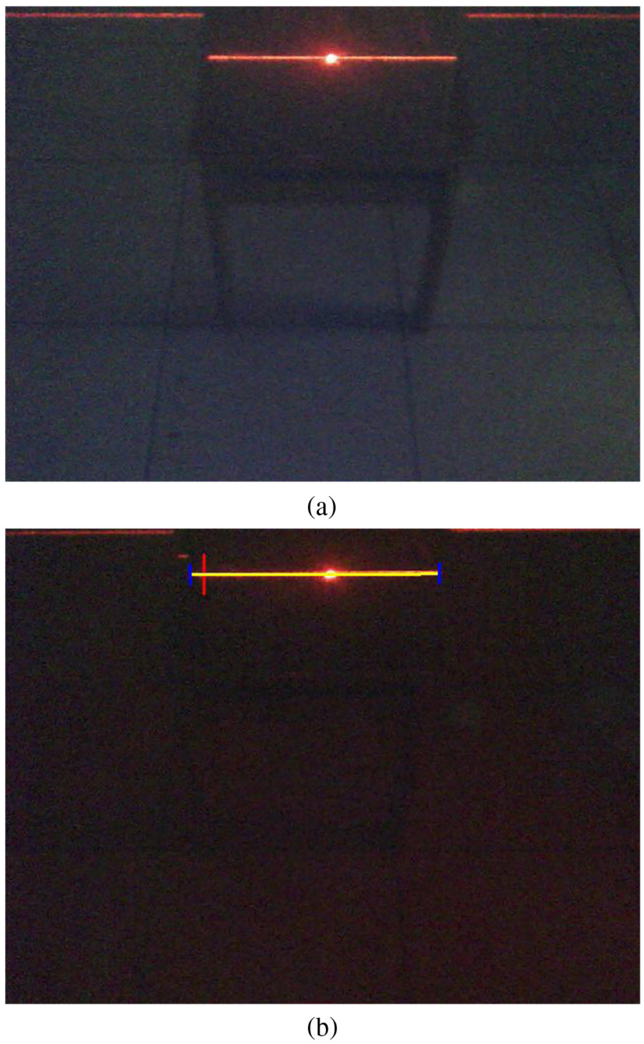

Fig. 9 The experimental image with the horizontal laser. (a) The actual image when the distance between the obstacle object and the guidance system is equal to 80 cm; (b) the marked image using the same distance (after the original image is processed).

image is (0, 0), and the coordinates of the last point (bottom right) on the image is (639, 479) in pixel.

3.1 *Horizontal Laser Experiment*

First, an experiment for evaluating the performance of horizontal laser was conducted. The carton was used as the obstacle object, and the coordinates of the object that was placed in different positions on the obtained images were recorded, respectively. The measured data was obtained by averaging 30 measurements in which the distance between the object and the guidance system increased 10 cm each time. The actual image taken from the experiment is shown in Fig. 9(a). The system searched the nearest light beam and found out the line segment endpoint. Then the coordinates and the width of the line segment could be obtained. The marked line image is shown in Fig. 9(b). The mean value of the Y-axis position (pixels) and the object distance (cm) is shown in Fig. 10. In this figure, curve 1 is under a static situation. This means that the user with the blind guidance system stood in a fixed position. By contrast,

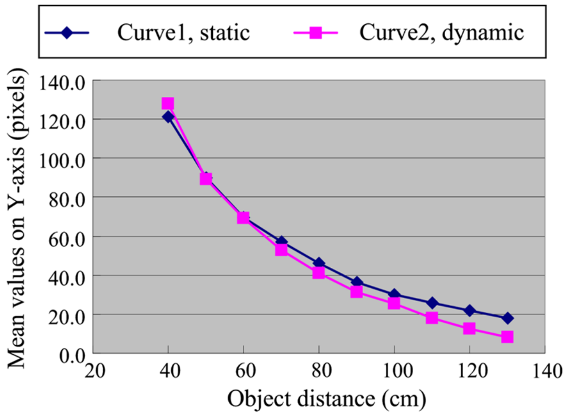

Fig. 10 Mean values (pixels) of the *Y*-axis position and the object distance (cm) with the horizontal laser.

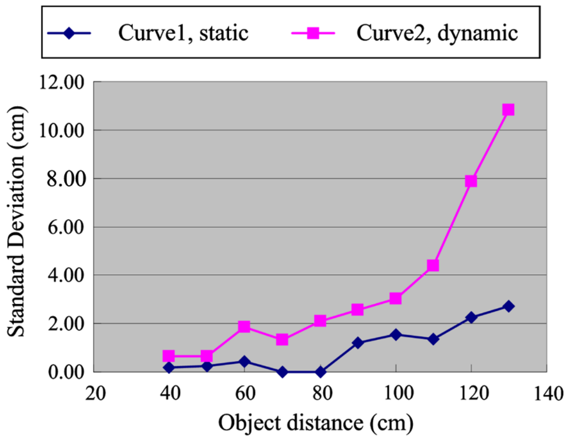

Fig. 11 Standard deviation (cm) of the measured distance and the object distance (cm) with the horizontal laser.

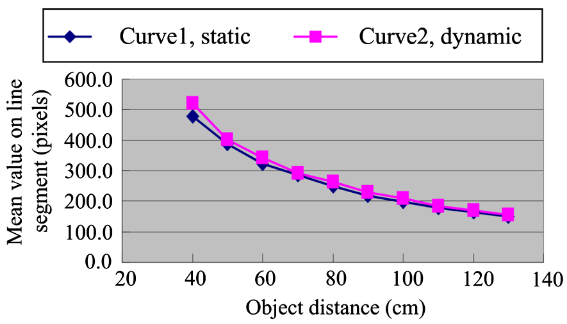

Fig. 12 Line segment (pixels) and the object distance with the horizontal laser.

curve 2 shows a dynamic situation where the user with the blind guidance system moved toward a predetermined position. Apparently, the deviation measured error increased, as shown by curve 2 in Fig. 11. The large deviation of curve 2 was caused by movement deviation. A smaller pixel deviation will result in a larger deviation during distance estimation, if the distance between the object and the guidance system becomes longer.

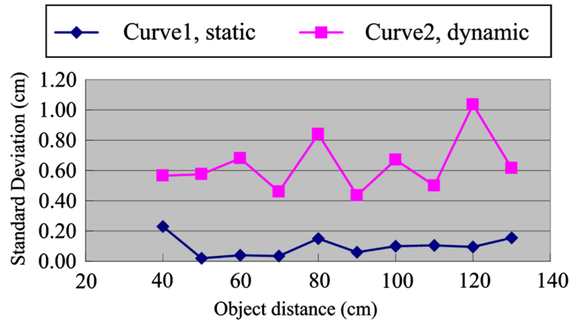

Fig. 13 Standard deviation (cm) of the measured object width and the object distance (cm) with the horizontal laser.

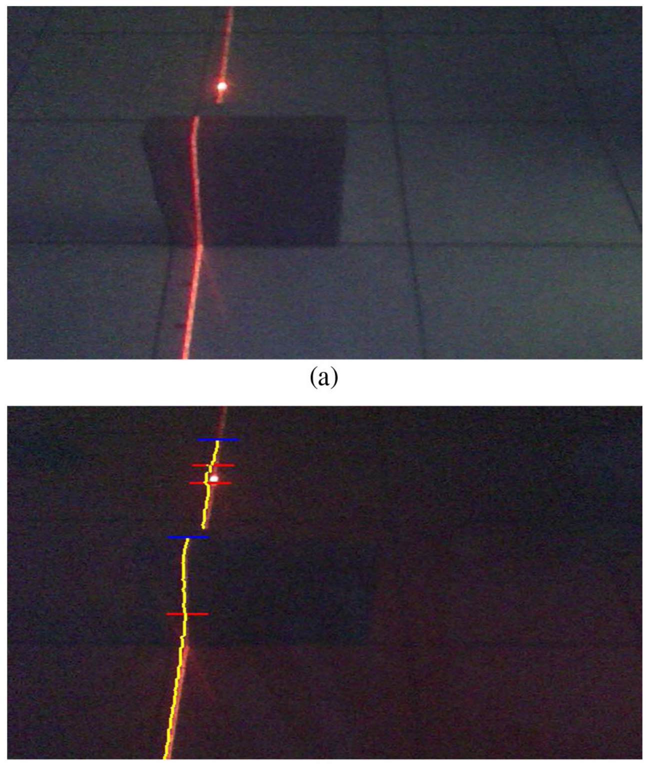

(a)

(b)

Fig. 14 The experimental image with the vertical laser. (a) The actual image when the distance between the obstacle object and the guiding system is equal to 80 cm; (b) the marked line using the same distance.

The maximum standard deviation (cm) of the measured distance for the static experiment is about 2.71 cm at a distance of 130 cm, as shown by curve 1 in Fig. 11. The maximum standard deviation (cm) of the measured distance for the dynamic experiment is about 10.82 cm at a distance of 130 cm, as shown by curve 2 in Fig. 11. The relations between the line segment (in the *Y* axis [pixels]) and the object distance are shown in Fig. 12. The maximum standard deviation (cm) of the object width for the static experiments is about 0.23 cm at a distance of 40 cm, as shown by curve 1 in Fig. 13. The maximum standard deviation (cm) of the object width for the dynamic experiments is about 1.04 cm at a distance of 120 cm, as shown by curve 2 in Fig. 13.

There is a particular light spot on the laser beam, as shown in Fig. 9(a). This is because the diameter of the rod lens is

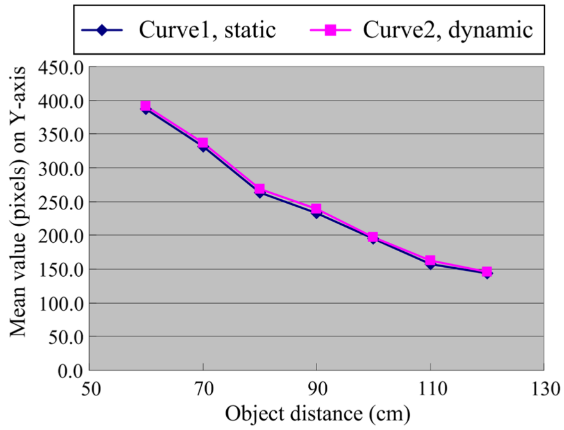

Fig. 15 Mean values (pixels) of Y-axis position and the object distance (cm) with the vertical laser.

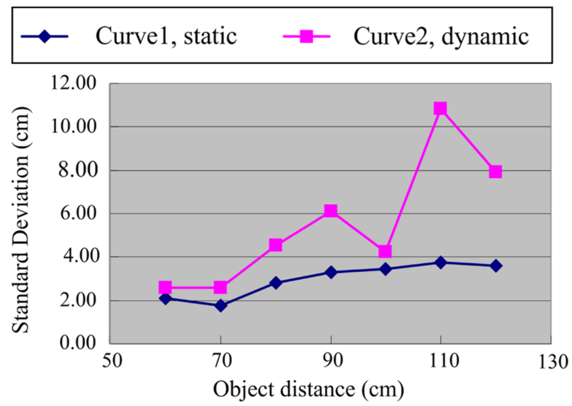

Fig. 16 Standard deviation (cm) of the measured distance and the object distance (cm) with the vertical laser.

smaller than that of the laser beam. Such a phenomenon can be overcome by choosing a larger diameter cylindrical lens.

3.2 *Vertical Laser Experiment*

Furthermore, a vertical laser experiment was conducted. The experimental settings and the measurement arrangement were the same as those in the horizontal experiment. Figure 14(a) shows the actual image taken from the vertical laser experiment. The guidance system searched the nearest turning point and breaking point so that the coordinates of the obstacle can be obtained. The marked line image is shown in Fig. 14(b). The mean value of the Y-axis position is shown in Fig. 15. The maximum standard deviation (cm) of the measured distance for the guidance system in static situation is approximately equal to 3.76 cm at a distance of 110 cm, as shown by curve 1 in Fig. 16. The maximum standard deviation (cm) of the measured distance for the guidance system in dynamic situation is approximately equal to 10.82 cm at a distance of 110 cm, as shown by curve 2 in Fig. 16.

4 Conclusions

A blind guidance prototype system designed for distance and obstacle width measurement is reported. According to the experimental results, the standard deviation of the measuring distance is below 8.5% within the range of 40 and 130 cm. The standard deviation of the object width, on the other hand, is less than 4.5% within the range of 40 and 130 cm. This guidance system could be used to assist the blind people with visual impairment to detect the situation in front of them. The designed guidance system also offers several advantages, including simple configuration, non-handheld design, and low costs.

In the future work, we will replace the visible laser with an infrared lase and implement our system on an embedded system to minimize the dimension of the entire system. In addition, GPS and compass module will be integrated into the proposed guidance system to display the location of user and direct the correct direction to user.

Acknowledgments

The authors are grateful to the National Science Council of the Republic of China for its financial support to this research under contract no. NSC 99-2221-E-130-002.

References

1. J. H. Wu et al., “Triangulation-based laser range finder using a complementary metal-oxide semiconductor image sensor for application to automotive systems,” *Opt. Eng.* **45**(4), 044302 (April 2006).
2. J. H. Wu, C. C. Pen, and J. A. Jiang, “Applications of the integrated high-performance cmos image sensor to range finders—from optical triangulation to the automotive field,” *Sensors* **8**, 1719–1739 (2008).
3. M. A. G. Izquierdo et al., “Sub-pixel measurement of 3-D surfaces by laser scanning,” *Sens. Actuators A: Phys.* **76**(1), 1–8 (1999).
4. Y. Bar-Shalom, H. M. Shertukde, and K. R. Pattipati, “Use of measurements from an imaging sensor for precision target tracking,” *IEEE Trans. Aero. Electron. Syst.* **25**(6), 863–872 (1989).
5. R. H. Stanton et al., “Optical tracking using charge-coupled devices,” *Opt. Eng.* **26**(9), 930–938 (1987).
6. L. J. Zeng et al., “A two-beam laser triangulation for measuring the position of a moving object,” *Opt. Lasers Eng.* **31**(6), 445–453 (1999).
7. G. Y. Wang et al., “Modeling and calibration of the laser beam-scanning triangulation measurement system,” *Robot. Auton. Syst.* **40**(4), 267–277 (2002).
8. R. T. Lee and F. J. Shiou, “Multi-beam laser probe for measuring position and orientation of freeform surface,” *Measurement* **44**(1), 1–10 (2011).
9. S. Shoval, J. Borenstein, and Y. Koren, “The NavBelt—a computerized travel aid for the blind based on mobile robotics technology,” *IEEE Trans. Biomed. Eng.* **45**(11), 1376–1386 (1998).
10. I. Ulrich and J. Borenstein, “The guide cane—applying mobile robot technologies to assist the visually impaired,” *IEEE Trans. Syst. Man Cybern. A Syst. Humans* **31**(2), 131–136 (2001).
11. J. Borenstein and I. Ulrich, “The guide cane—applying mobile robot technologies to assist the visually impaired,” *Proc. IEEE International Conference on Robotics and Automation*, Albuquerque, NM, 1283–1288 (April 21–27 1997).
12. S. Tachi and K. Komority, “Guide dog robot,” *2nd Int. Congress on Robotics Research*, Kyoto, Japan, 333–340 (1984).
13. I. Ban and Y. Mitsuta, “Blind Person Guide Device,” United States Patent, US 4,712,003 (December 8 1987).

Jih-Huah Wu received his PhD in optical sciences at National Central University in 2005. After serving as one-year post doctoral fellow in the Department of Power Mechanical Engineering in the National Tsing Hua University, he joined Ming Chun University and served as an assistant professor at the Department of Biomedical Engineering. He became an associate professor in 2010. His research interests include electro-optical system design, laser acupuncture, light therapy, and the applications of semiconductor lasers in biomedical researches.

Jinner-Der Wang received his PhD in electrical engineering from the National Central University, Taiwan, in 1995. He is currently an associate professor at the Department of Computer Science &

Information Engineering, St. John's University, Taiwan. He is interested in intelligent control systems and embedded systems design.

Wei Fang received his PhD at the Department of Biological and Agricultural Engineering, Rutgers University, USA, in 1989 and worked as post-doctoral researcher at Center of Excellence for Controlled Environment Agriculture (CCEA) in the same University until 1992. Then he was hired as an associate professor at the Department of Agricultural Machinery Engineering, National Taiwan University, where he got his BS and MS. He was promoted to professor in 1996. In 1998, the department changed name into Department of Bio-Industrial Mechatronics Engineering. His research in recent decade related to several topics including: (a) Applications of dual effect air conditioning/heat pump in bio-industries. (b) Applications of hypo-chlorous water with high free active chlorine (FAC) concentration generated by membrane-less traceability of agricultural produces. (e) Development of plant factory platform for research and mass production of leafy greens.

Yun-Parn Lee received his MSEE and MS in mathematics from University of Cincinnati in 1979 and 1980, *Who's Who in Science and Engineering*, 4th edition, 1998–1999. During his career, Lee has worked for SONY, Philips, NEC, and SST. Lee is currently an Assistant Professor of Department of Electronic Engineering, Ming Chuan University, Taoyuan, Taiwan, Republic of China.

Yi-Chia Shan was born in Taoyuan County, Taiwan, ROC, on February 8, 1971. He received the BE in 1993 from the Department of Electrical Engineering, National Taiwan Ocean University. He received the ME in 2008 from the Graduate Institute of Communication Engineering, Taiwan Tatung University. Now he is working in the Marketech International Corporation. Additionally, he is studying toward his PhD at National Taiwan University. His major research subjects are optical medical device and embedded systems.

Hai-Ko Kao received his BS in computer science and information engineering from St. John's University, Taiwan, in 2010. Now he is a master student of computer science and information engineering of St. John's University. His research interests include embedded system software program design.

Shih-Hsin Ma received his PhD in optical sciences from National Central University in 2007. In 2010, he joined the Department of Photonics of the Feng Chia University, Taiwan, and became an assistant professor at the Graduate School of Photonics. His research interests are solid-state lighting design, laser beam shaping, optical design in PV systems, and random phase multiplexing in volume holograms.

Joe-Air Jiang received the PhD degrees in electrical engineering from National Taiwan University, Taiwan in 1999. Currently, he is a Professor of Bio-industrial Mechatronics Engineering at National Taiwan University, Taiwan. He is an active researcher. He was the recipient of the Annual Best Paper Award from Taiwan Society of Naval Architects and Marine Engineers in 2010 and the Academic Achievement Award from Chinese Institute of Agricultural Machinery in 2010. He is the principal investigator of several large-scale integration projects funded by the National Science Council, the Council of Agriculture of the Executive Yuan, and Intel-NTU Connected Context Computing Center. His specialties in power transmission system are computer relaying, solar generation system, power quality event analysis, and smart grid system. Besides, his areas of interest are diverse that cover wireless sensor network technology, bio-mechatronics, bio-effects of electromagnetic wave, automatic system for agroecological monitoring with WSN, and low-level laser therapy.